COBEM 2023 27TH INTERNATIONAL CONGRESS OF MECHANICAL ENGENEERING

ABCM Brazilian Society of Mechanical Sciences and Engineering
27th ABCM International Congress of Mechanical Engineering
December 04-08, 2023, Florianópolis-SC, Brazil

COB-2023-0097

EXPERIMENTAL APPRAISAL OF LONG-TERM DEGRADATION OF PV MODULES IN RIO DE JANEIRO

Félix do Rêgo Barros
Centro Federal de Educação Tec. Celso Suckow da Fonseca –Maria da Graça (CEFET/RJ)
Programa de Pós-Graduação em Engenharia Mecânica (PPG-EM) Universidade do Estado do Rio de Janeiro (UERJ)
felix.barros@cefet-rj.br

Ebenézer Viana Oliveira
Felipe Rodriguez Franklin
Programa de Pós-Graduação em Engenharia Mecânica (PPG-EM) Universidade do Estado do Rio de Janeiro (UERJ)
ebenezer.viana@hotmail.com
felipefranklin07@gmail.com

Sebastião Fabio Quintiliano de Araújo Rocha
Centro Federal de Educação Tec. Celso Suckow da Fonseca –Maria da Graça (CEFET/RJ)
sebastião.rocha@cefet-rj.br

Manoel Antônio da Fonseca Costa Filho
Programa de Pós-Graduação em Engenharia Mecânica (PPG-EM) Universidade do Estado do Rio de Janeiro (UERJ)
costafh@uerj.br

Abstract. *The State University of Rio de Janeiro has a photovoltaic installation located in the São Cristóvão neighborhood in Rio de Janeiro city. It has continuously operated in the off-grid mode since 2007. The fifteen-polycrystalline silicon modules BP MSX120 are north-oriented with an inclination of 32°, above the local latitude of 22°30', resulting in a higher energy production in the winter, the driest season, added by less PV module heating. This study focuses on the DC circuit of seven modules, isolated to feed a purely resistive load. This paper experimentally evaluates the impact of the climatic conditions on the degradation of these modules, expressed as power loss at the maximum power point at Standard Test Conditions, after 16 years of operation. A supervisory developed in LabView has continuously recorded in a minute base, the incident global solar radiation, atmospheric relative humidity, ambient and shaded surface PV module temperature, individual and total module currents, and array voltage, as all modules are connected in parallel. Literature reported that hot and humid climates promote the highest PV degradation rates, pronounced in those manufactured until 2010. In-site previous studies found annual degradation rates up to 2.5%. Soiling was included in degradation since there is no active cleaning here, as in almost Brazilian rooftop PV installations. Natural random cleaning by the rain and wind limits dirt deposition in high-rainfall sites. Overall degradation has overcome the manufacturer's warranty of power loss of up to 20% after 20 years of operation. This paper ends highlighting the need to use real yearly degradation rates in feasibility studies for PV generation, and the low availability in the literature of long-term experimental appraisal of PV module performance in hot and humid climates.*

Keywords: *photovoltaic modules, PV aging, degradation, long-term experimental appraisal*

1. INTRODUCTION

Photovoltaic (PV) module aging is a relevant factor to be considered when performing economic feasibility appraisals. Information on the long-term reliability of PV modules installed in tropical regions is limited (Luo et al., 2018). (Jordan and Kurtz, 2013); (Jordan et al., 2016); (Golive et al., 2019) observed that modules deployed in hot and humid climates degrade at a higher rate than in other climates. Aging and dirty promote a lumped effect in power loss on PV installations. Although some experimental evaluations of losses produced by soiling in Brazil are available in the literature (Tonini et al., 2013); (Hickel, 2017); (Barros et al., 2019); (Alves, 2018); (Barbosa et al., 2018), this information cannot be reliably translated to the specific site of interest because the accumulation of dirt strongly depends on the site. Therefore, it is impractical to separate their effects when attempting to estimate the actual energy production of PV installations.

PV degradation reports in Brazil are scarce in the literature. (Rüther and Dacoregio, 2000) presented the monitoring results of the first eighteen working months of a 2-kWp on-grid system composed of a-Si panels installed in Florianópolis, in the Brazilian Temperate Zone. (Ruther et al., 2003) extended this information to 5 years, graphically showing a slight decrease in performance in time evolution. (Vera et al., 2006) found a reduction of 6% and 4% in power output from 8 off-grid PV modules, respectively, due to aging and dust deposition, after comparing I-V curves measured at starting operation and six years later in continuous running in Porto Alegre, another Brazilian city situated within the Temperate Zone.

(Fonseca et al., 2020) analyzed the aging of a 48-module system operating for 15 years in Porto Alegre, Brazil. They found a 9.50% loss in the average installation power, corresponding to a yearly average of 0.7%, attributing most of the power loss to current reduction (9.19% and 9.12% for current at the maximum power point [I_{mp}] and short-circuit current [I_{SC}], respectively).

This paper experimentally evaluates the impact of the climatic conditions on the degradation of five PV modules from the same installation, expressed as power loss at the maximum power point at Standard Test Conditions, after 16 years of operation in the city of Rio de Janeiro. Besides the tropical climate, the studied site is close to the sea and the urban pollution must also be considered in the weathering effect on the PV modules.

2. THEORETICAL MODEL

The use of the single-diode model (SDM) to represent the current-voltage characteristics of a PV module is well consolidated in the literature (Villalva et al. 2009); (Brano et al., 2010); (Duffie and Beckman, 2013); (Doumane et al., 2015); (Kumar and Kumar, 2017a, 2017b). According to Kirchhoff's laws, its I-V characteristics can be mathematically expressed by "Eq. (1)" (Huang and Wang, 2018).

$$I = I_{ph} - I_0\left(e^{\frac{V+IR_s}{V_T.a}} - 1\right) - \frac{V + IR_s}{R_{sh}} \tag{1}$$

Where the variables are photocurrent [I_{ph}], series resistances [R_s], shunt resistances [R_{sh}], dark saturation current [I_0], diode ideality factor [a], output current [I], output voltage [V] and Boltzmann constant [k], cell temperature [T], electronic charge [q], and the thermal equivalent voltage [V_T] as expressed by "Eq. (2)".

$$V_T = \frac{N_s kT}{q} \tag{2}$$

This mathematical model of the PV module that describes the relationship between voltage and current is a nonlinear and implicit equation with five unknown parameters (Piliougine et al., 2021a). Additionally, "Eq. (1)" requires corrections to include the influence of the cell temperature [T] and solar irradiance [G] on its variables. (Ibrahim, H., and Anani, N., 2017) present and discuss the most common expressions used in the literature for this purpose. The simplest formula that reaches the desired accuracy must be chosen.

"Equation (3)" relates the temperature of cells inside the module and the module back surface temperature [T_m], assuming one-dimensional heat conduction through the module (King et al., 2004). In "Eq. (3)", [ΔT_1] represents this difference at an irradiance level of 1,000 W/m^2 [G_{STC}]. (King et al., 2004) found three °C for this temperature difference for flat-plate polycrystalline-silicon modules in an open-rack mount.

$$T = T_m + \frac{G}{G_{STC}}\Delta T_1 \tag{3}$$

The assumption $I_{ph} = I_{sc}$ is generally used in photovoltaic models. From a practical point of view, the value provided by the sensor may not represent the effective irradiance received by the PV module; therefore, the approximation of I_{ph} through a direct measure of I_{sc}, according to the effective operating conditions of the module, is commonly used (Bastidas-Rodriguez et al., 2017).

$$I_{ph}(G,T) = I_{sc}(G,T) = \frac{G}{G_{STC}}\left[I_{sc,STC} + k_i(T - T_{STC})\right] \tag{4}$$

The open-circuit voltage [V_{oc}]exhibits a strong dependence on *T*, described by temperature coefficient of open-circuit voltage [k_v], and a not very significant logarithmic dependence on *G* (Duffie and Beckman, 2013). "Eq. (5)" neglects the influence of *G* (Villalva et al., 2009).

$$V_{oc}(T) = V_{oc,STC} + k_v(T - T_{STC}) \tag{5}$$

(Sera and Rodriguez, 2008) and (Chatterjee et al., 2011) reported a strong temperature dependence of I_0. Assuming an infinite value for R_{sh} and the mentioned approximation of I_{ph} by I_{sc} from "Eq. (1)" at the open circuit point leads to "Eq. (6)" (Villalva et al., 2009; Can et al., 2012; Chegaar et al., 2013).

$$I_0 = \frac{I_{sc,STC} + k_i(T - T_{STC})}{e^{\left(\frac{V_{oc,STC}+k_v(T-T_{STC})}{a.V_T}\right)} - 1} \tag{6}$$

R_s was assumed constant while R_{sh} is independent of T and varies linearly with G, as expressed by "Eq. (7)" (Soto and Beckman, 2006; Chegaar et al., 2013; Duffie and Beckman, 2013).

$$R_{sh}(G) = \left(\frac{G_{STC}}{G}\right) R_{sh,STC} \tag{7}$$

Finally, the current output is determined by "Eq. (8)", formed after grouping "Eq. (1), (4), (6), and (7)".

$$I = \frac{G}{G_{STC}}\left[I_{sc,STC} + k_i(T - T_{STC})\right] - \frac{I_{sc,STC} + k_i(T - T_{STC})}{e^{\left(\frac{V_{oc,STC}+k_v(T-T_{STC})}{V_T.a}\right)} - 1}\left(e^{\frac{V+I.R_{s,STC}}{V_T.a}} - 1\right) - \frac{V + I.R_{s,STC}}{\left(\frac{G_{STC}}{G}\right) R_{sh,STC}} \tag{8}$$

"Equation (8)" has five unknown parameters that are cannot be directly determined. A comprehensive review of the methods for extracting the parameters of the SDM can be seen in (Chin et al., 2015). (Rodrigues Junior, J. and Maciel, 2021) present the optimization technique employed here. The values of R_s, $R_{sh,}$ and a found through minimizing the sum of the differences of the squared theoretical and measured currents by optimization were used to calculate the present current and voltage corresponding to the maximum power point at each minute. This was required because of the lack of a maximum power point tracker.

3. EXPERIMENTAL SETUP

The Center of Studies and Researches in Renewable Energies (CEPER) was established at the Rio de Janeiro State University's Campus located in the São Cristóvão neighborhood in the city of Rio de Janeiro in 2006 through the financial support of the State Government. It intermediated with BP Solar the donation of fifteen polycrystalline silicon modules BP MSX120, which included the inverters and battery charge controllers. Lead acid batteries donated by Batteries Moura complemented this off-grid PV system. CEPER executed all design of the supporting frame and mounting and wiring of the PV system. The PV modules were installed in 2007 fixed on a metallic frame north-oriented with an inclination angle of 32°, above the local latitude of 22°30', resulting in a higher energy production in the winter, the driest season, added by less PV module heating. The initial uses were demonstration of the PV technology and researches on recharging of electric vehicle batteries. "Table 1" shows the BP MSX 120 characteristics.

Table 1. BP MSX 120 characteristics, from manufacturer datasheet

PV Module characteristic	Value
Maximum power (Pmax)	120 W
Voltage at Pmax (Vmp)	33.7 V
Current at Pmax (Imp)	3.56 A
Short-circuit current (Isc)	3.87 A
Open-circuit voltage (Voc)	42.1 V
Temperature coefficient of Isc	(0.065 ± 0.015) %/ ºC
Temperature coefficient of Voc	-(80±10) mV/ ºC
Temperature coefficient of power	-(0.5±0.05) %/ ºC
Normal operating cell temperature	47±2 ºC
Efficiency	10.9%

The monitoring to study PV module degradation has started in 2017. Seven PV modules were arranged to compose a DC circuit by parallel connecting them to feed a purely resistive load. Unfortunately, module number 5 was out of service during the investigation period. This subset has been continuously monitored through real-time measurements at 1-second intervals and successively stored as 1-minute averages. A supervisory has recorded the global solar irradiation, illuminated, and shaded PV module's surfaces and ambient temperatures, the currents of each PV module, the total current, the voltage of the PV array and the air relative humidity. (Barros et al., 2019). Table 2 shows all sensor descriptions. The supervisory was developed in LabVIEW using Compact Field Point as external computer interface, both from National Instruments Inc. Compact Field Point is a programmable logic controller in a modular architecture, supported by specific signal conditioner cards mounted in accordance with the user's needs. Five TC-120 cards receive signals from thermocouples and

two AI-110 cards read the other sensors. (Barros et al., 2019). The modules were enumerated. The first two have four temperature sensors in each face, totaling sixteen temperature recordings. The others have temperature sensors only on their shaded surface. Thermal paste was used between the sensors' surface and the module surface to ensure good thermal contact. In addition, aluminum adhesive tape has also been used to fix sensors and shield them from thermal irradiation, avoiding overestimating surface temperature.

Table 2. Sensors used, reproduced from (Soares et al., 2017)

Type	Manufacturer	Model	Range	Precision / sensibility
Thermocouple - T type	Thermomax	TP 3279	0 ºC to 370 ºC	±1.0 ºC
Current transmitter	SECON	05T420ADC-24VDC	0 to 5ADC	±1 %
Current transmitter	SECON	35C420ADC-24VDC	0 to 35ADC	±1 %
Voltage transmitter	SECON	50V420ADC-24VDC	0 to 50VDC	±1 %
Solar irradiation	Kipp and Zonen	CMP3	0 to 2000W/m²	5 to 20 µV/W/m²

The experimental data used in this research were collected between April 18th. and May 24th, corresponding to 18,766 simultaneous measurements of all climatic and electric variables at a minute-based frequency. All PV modules were daily checked for the quality of adhesion of their temperature sensors and to ensure that there were substantial particles on neither their illuminated surfaces nor the irradiance sensor, such as bird droppings. A low irradiance threshold of 50 W/m² was imposed due to the limitation of the accuracy of the pyranometer. In contrast, no superior threshold was applied since the observed cloud reflections were short-term phenomena, smoothed by minute-averaged records, with low frequency in the dataset. Additionally, the data were excluded whenever the measured current was higher than the [I_{sc}] calculated by "Eq. (4)".

Measuring the [V_{OC}] and [k_v] was performed. The module under test was isolated from the others by opening its circuit breakers, and its terminals remained open. Both the module and the pyranometer were previously cleaned. Continuously measured data were filtered for irradiance within (1,000 ± 20) W/m². Only data with temperature differences less than 3°C between any back module thermocouples were included to approximate an isothermal condition for the module cells, following the recommendation of IEC 60981. For approaching steady-state conditions, the average measured back-module temperatures in the last three minutes could not exceed 0.5°C. Data filtering can significantly improve precision during photovoltaic field tests by restricting the analysis to well-defined measurement conditions (Carlsson et al., 2006). By filtering, the outdoor conditions could approximate the controlled indoor conditions. The cell temperature was calculated by "Eq. (3)", using the average of the measured temperatures of the back surface. Plotting [V_{oc}], as the dependent variable and the difference between the measured cell and the T_{STC} as the independent variable, the intercept corresponds to [V_{oc}] and the slope to [k_v]. They were obtained from a least-square linear regression of measured data. The measured [I_{sc}] at the end of 2020 and the k_i from the module's datasheet "Table 1" were adopted here, due to time and experimental limitations, respectively. (Piliougine et al., 2021b) present a full background of difficulties in outdoor measuring of k_i.

4. RESULTS

"Table 3" presents the measured [V_{oc}] and [k_v]with their respective goodness of fit and the number of points used in the least squares regression to find [V_{oc}] and [k_v]. [I_{SC}] measured in the end of 2020 was added in "Table 3". "Figure 1" illustrates the graphical determination of [V_{oc}] and [k_v].

Table 3 I_{SC}, V_{oc} and k_v with their regression goodness of fit for V_{oc}/k_v

PV Module	I_{SC} (A)	V_{OC} (V)	k_v (V/°C)	Adjusted R-squared (V_{OC}/k_v)	Number of points (V_{OC}/k_v)
1*	3.31	41.0	-0.137	0.9519	53
2*	3.28	40.9	-0.151	0.9782	36
4	3.31	41.2	-0.148	0.9920	115
6	3.36	40.5	-0.145	0.9898	47
7	3.31	40.1	-0.128	0.9662	106

(*) with four thermocouples installed on its illuminated surface.

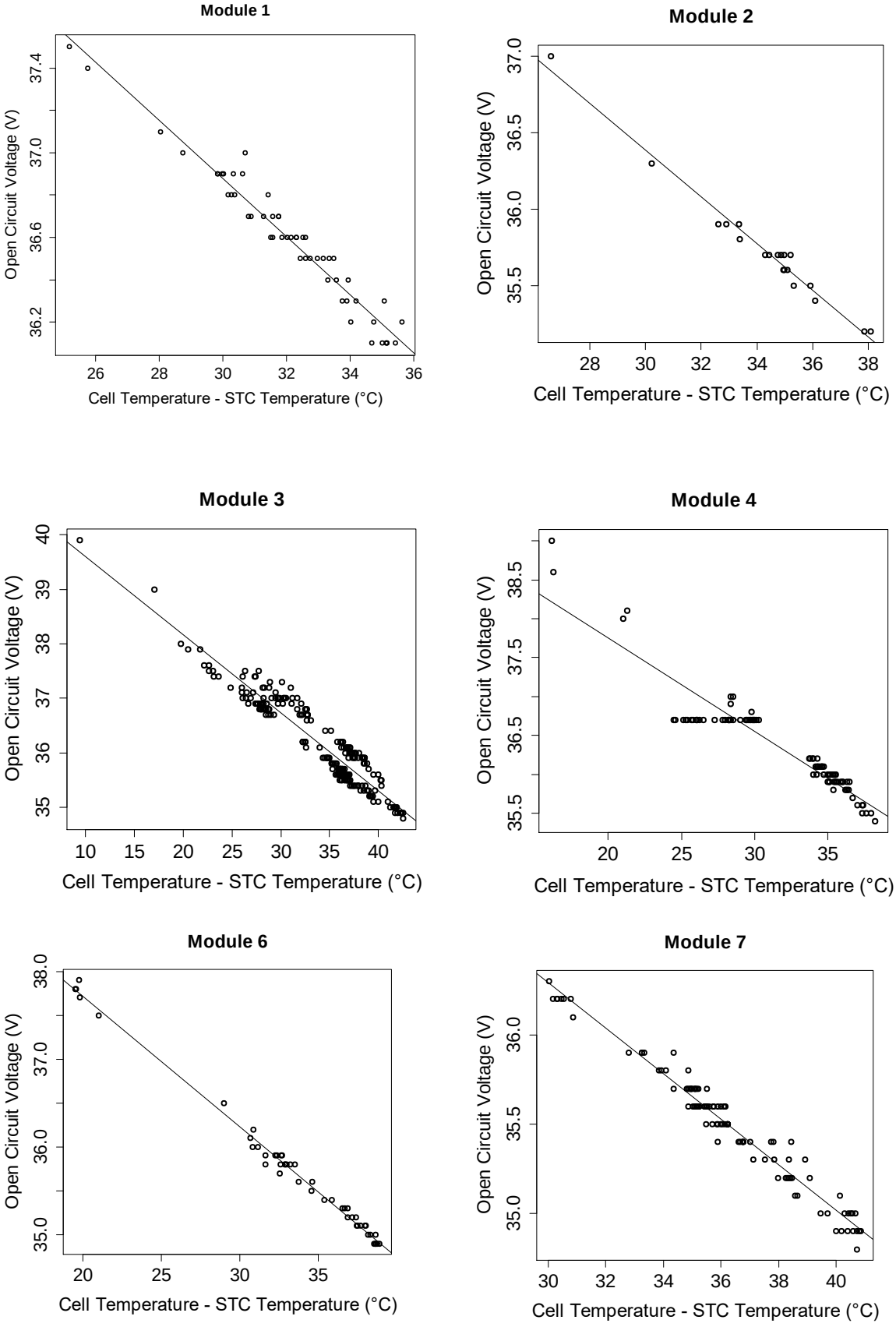

Figure 1. Graphical determination of V_{oc} and k_v for each module.

"Table 4" presents R_s, R_{sh}, and a found by the optimization procedure and the relative errors in the current output. The low errors obtained after comparing measured with predicted current has proved the adequacy of the parameters found to represent the PV module power output.

Table 4 Model parameters and relative errors in current output.

Module	Parameters			Relative error in current output			
	R_s (Ω)	R_{sh} (Ω)	a	mean	1st quartile	Median	3st quartile
1*	1.142	68.11	1.097	0.20%	-0.02%	0.02%	0.04%
2*	0.867	60.38	1.204	0.00%	-0.03%	0.00%	0.04%
4	1.184	109.32	1.123	0.21%	-0.02%	0.01%	0.04%
6	0.74	61.45	1.175	0.00%	-0.02%	0.02%	0.04%
7	0.856	58.52	1.037	0.00%	-2.54%	-0.12%	0.04%

(*) with four thermocouples installed on its illuminated surface.

After finding the R_s, R_{sh}, and a, it was possible to trace the updated I-V and P-V curves at STC for each degraded module ("Figure 2") and locate the corresponding P_{mp}. The overall degradation was calculated by the difference between P_{mp} and the maximum power from the manufacturer's datasheet ("Table 1") divided by the latter. This calculation assumes that all modules were sold with power characteristics exactly as declared in the datasheet. This is reasonable because all units are tested in the factory, and those that do not achieve the minimum required power output are classified as 110 W models. Additionally, a uniform yearly degradation rate was calculated. "Table 5" presents overall degradation and their annual rate for all PV modules, besides their I_{mp}, V_{mp} and P_{mp}.

Table 5. P_{mp} overall degradation, and annual degradation rate.

PV Module	I_{mp} (A)	V_{mp} (V)	P_{mp} (W)	Overall Degradation	Yearly Degradation Rate
1*	2.675	32.28	86.63	27.81%	2.02%
2*	2.608	32.22	84.04	29.97%	2.20%
4	2.839	32.04	90.99	24.17%	1.71%
6	2.684	32.48	87.17	27.36%	1.98%
7	2.645	31.99	84.64	29.47%	2.16%

(*) with four thermocouples installed on its illuminated surface.

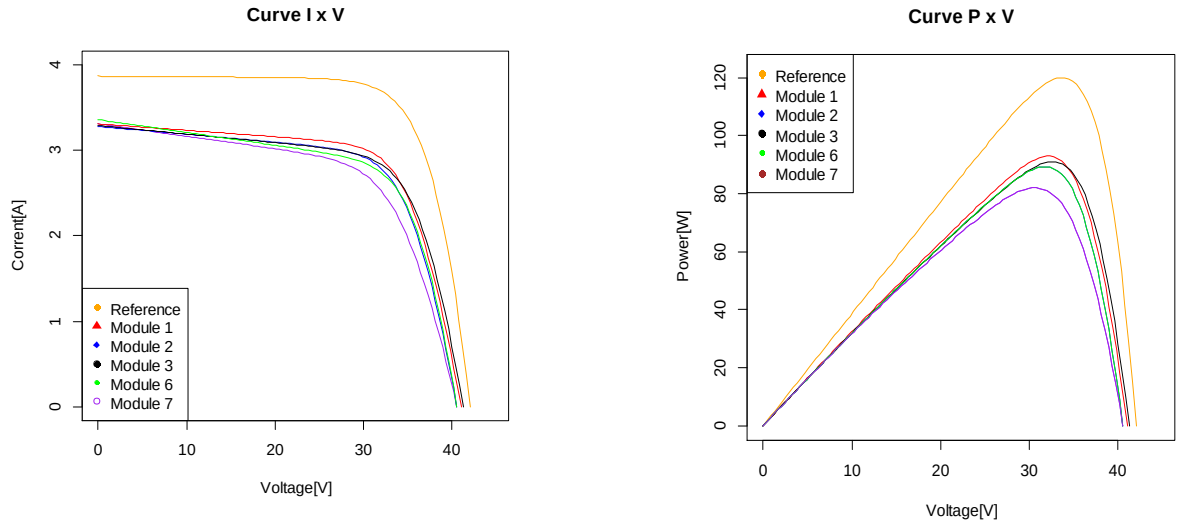

Figure 2 - I-V and P-V curves at STC

"Table 6" summarizes the degradation rates reported in the literature for p-Si PV modules in hot and humid climates. The yearly degradation rates follow the PV modules that started operating until 2010 in Table 6, except for the 19-year evaluation in Ghana. (Nascimento et al., 2019) reported intense degradation of crystalline silicon modules in areas with high relative humidity and temperature in Brazil. (Jordan and Kurtz, 2013, 2016) mentioned that module warranties increased accordingly, and module durability increased in the decades 1980-90, 1990-2000, and 2000-2010. It is worth noting that soiling was computed jointly with degradation, but the higher rainfall of the tropical climate diminishes its effects. The soiling losses are maintained below 10% for glass-surfaced modules due to self-cleaning by wind and rain (Meyer and Dyk, 2004).

Table 6 Degradation rates of p-Si PV-modules in hot and humid climates.

References	Place	Years of Aging	Yearly Degradation Rate
Sastry et al. (2010)	India	10	2.5%
Sorloaica-Hickman et al. (2012)	Florida, United States	5	2.5%
Ndiaye et al. (2014)	Dakar, Senegal	4	2.96%
Ye et al. (2014)	Singapore	3	1%
Limmanee et al. (2017)	Thailand	4	1.2%
Quansah et al. (2017)	Ghana	19	1.3%
Islam et al. (2018)	Kuala Lumpur, Malaysia	9	1.89%
Luo et al. (2018)	Singapore	7	0.46%

Traditionally, the condition of PV modules is assessed in the field using an I–V curve tracer, which provides an instantaneous picture. To illustrate the limitations of this method in accurately representing the actual performance of a degraded PV module during operation, the I–V curve of module number 13 was obtained using the HT Instruments SOLAR I–Ve device. The data presented in "Table 7" indicates a higher level of degradation than that evaluated above. This difference can be attributed to several factors, including variations in aging among modules within the same PV system with identical weathering exposure and, primarily, the limitations associated with the instantaneous evaluation of module performance. Given the on-site unavailability of an I–V curve tracer and the safety risk of circulating with one due to its high cost, one unmonitored module was removed and sent to another university to be assayed.

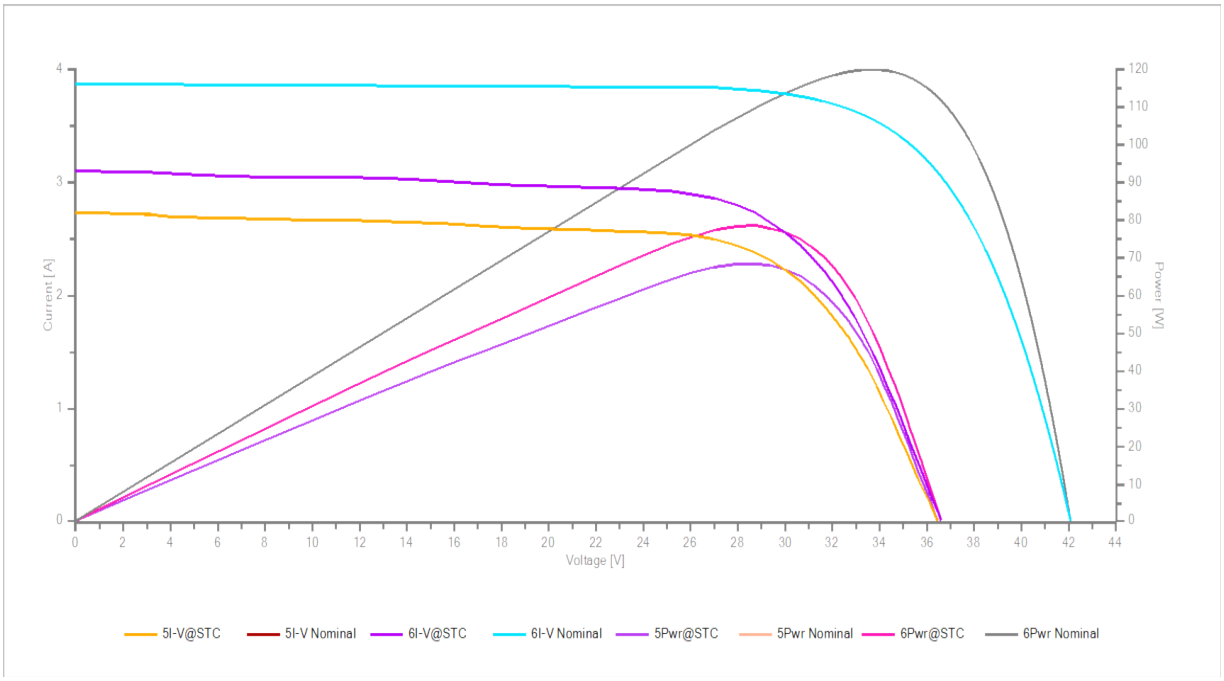

Figure 3. Curves *I-V* and *P-V* of module number 13, obtained through an I-V tracer.

Table 7 Data obtained by an I-V tracer for module number 13,

	Pmax [W]	Voc [V]	Vmpp [V]	Impp [A]	Isc [A]	Irrad. [W/m2]	Module Temp.[°C]
Meas. 5 - BPMX 120 UERJ 06/06/2023 14:11	Not Ok (-43.05%)						
5 Measures@OPC	48.07	36.43	28.64	1.68	1.92	703	35.0
5 STC	68.35	36.49	28.66	2.38	2.72	1000	25.0
Meas. 6 - BPMX 120 UERJ 06/06/2023 14:21	Not Ok (-34.59%)						
6 Measures@OPC	48.27	36.55	28.76	1.68	1.91	614.00	35.0
6 STC	78.50	36.61	28.75	2.73	3.09	1000.00	25.0

5. CONCLUSIONS

This study assessed the degradation of five polycrystalline silicon modules after 16 years of exposure in an open area. A LabVIEW-based supervisory system was employed to measure and record the power output and environmental variables at a minute-based frequency. Because of the lack of a maximum power point tracker, the maximum power output was determined at each minute using the SDM. The optimization technique used to derive the values of the five parameters in the SDM has proven effective, as evidenced by the low errors found in predicting the current output in the period considered.

The hot and humid climate of Rio de Janeiro accelerated the degradation of these PV modules, a climate type reported as the most aggressive in the literature. The annual degradation rates observed in this study aligned with the published degradation rates of PV modules manufactured during 2000–2010 under similar climate. Overall degradation has overcome the manufacturer's warranty of power loss of up to 20% after 20 years of operation.

This study has the following limitations: (1) the minimum required sampling period was not previously established. Data acquisition was conducted over 36 days, resulting in 18,766 usable simultaneous measurements of all variables of interest. Seasonal variation in SDM parameters has been reported in the literature based on experimental studies. Nevertheless, the present approach represents a significant improvement over the conventional method of instantaneously evaluating PV module performance using an I–V curve tracer. (2) Soiling was included in degradation because there is no active cleaning, as in almost Brazilian rooftop PV installations. Natural random cleaning by rain and wind limits dirt deposition at high rainfall sites.

The literature requires studies on the long-term experimental appraisal of PV module performance in hot and humid climates since real yearly degradation rates are requested in feasibility studies for PV generation. This study provided photovoltaic manufacturers with information on degradation losses as feedback for quality improvement, highlighting the need for special attention to application in hot and humid climates of the tropical zone.

6. ACKNOWLEDGEMENTS

This study was financed in part by the Coordenação de Aperfeiçoamento de Pessoal de Nível Superior – Brasil (CAPES) – Finance Code 001.

7. REFERENCES

Alves, F. R. R. Estudo do efeito da sujidade na eficiência de módulos fotovoltaicos. Dissertação de mestrado, Pontifícia Universidade Católica de Goiás. (2018).

Barbosa, E.R., Bandarra Filho, Faria Merlim, S.F., Gontijo Fabio, B., 2018. "Influence Of Dirt in Photovoltaic Generation" VII Congresso Brasileiro de Energia Solar *CBENS 2018*. Gramado, Brazil.

Barros, F.R., Costa Filho, M.A.F., Coutinho Junior, L.C., and Soares, D.R.M., 2019. Evaluation of the efficiency loss of photovoltaic modules due to urban dirt - a case study. In: COBEM 2019, 25th International Congress of Mechanical Engineering. https://doi.org/10.26678/ABCM.COBEM2019.COB2019-2222 Uberlândia, MG, ABCM. (2019)

Bastidas-Rodriguez, J.D. & Petrone, G. & Ramos-Paja, C.A. & Spagnuolo, G., 2017. "A genetic algorithm for identifying the single diode model parameters of a photovoltaic panel," Mathematics and Computers in Simulation (MATCOM), Elsevier, vol. 131(C), pages 38-54.

Brano, V.L., Orioli, A., Ciulla, G., and Di Gangi, A., 2010. An improved five-parameter model for photovoltaic modules. Solar Energy Materials and Solar Cells, 94 (8), 1358–1370. http://dx.doi.org/10.1016/j.solmat.2010.04.003.

Can, H., Ickilli, D., and Parlak, K.S., 2012. A new numerical solution approach for the real-time modeling of photovoltaic panels. 1–4. http://dx.doi.org/10.1109/APPEEC.2012.6307160.

Carlsson, T., Åström, K., Konttinen, P. and Lund, P., 2006. Data filtering methods for determining performance parameters in photovoltaic module field tests. Progress in Photovoltaics: Research and Applications, 14 (4), 329–340. http://dx.doi.org/10.1002/pip.669.

Chatterjee, A., Keyhani, A. and Kapoor, D., 2011. Identification of photovoltaic source models. IEEE Transactions on Energy Conversion, 26 (3), 883–889. https://doi.org/10.1109/TEC.2011.2159268.

Chegaar, M., Hamzaoui, A., Namoda, A., Petit, P., Aillerie, M., and Herguth, A., 2013. Effect of illumination intensity on solar cells parameters. Energy Procedia, 36, 722–729. http://dx.doi.org/10.1016/j.egypro.2013.07.084.

Chin, VJ, Salam, Z, and Ishaque, K., 2015. Cell modelling and model parameters estimation techniques for photovoltaic simulator application: A review. Applied Energy, 154, 500–519. http://dx.doi.org/10.1016/j.apenergy.2015.05.035

Doumane, R., Balistrou, M., Logerais, P., Riou, O., Durastanti, J., and Charki, A., 2015. A circuit-based approach to simulate the characteristics of a silicon photovoltaic module with aging. Journal of Solar Energy Engineering, 137 (2). https://doi.org/10.1115/1.4029541

Duffie, J. A., Beckman, W. A., Design of Photovoltaic Systems, Chapter 23 (2013).

Hickel, Bernado M., 2017. "The Impact on The Performance of Photovoltaic Systems Caused by The Dirt Acumulum On The Fv Module - Methodology and Evaluation Through IxV Field Curves". Dissertation, Federal University of Santa Catarina, Florianópolis, Brazil, 2017. (In Portuguese)

D. L. King, W. E. Boyson, J. A. Kratochvil Photovoltaic System R&D Department Sandia National Laboratories Box 5800 Albuquerque, New Mexico 87185-0752, 2004.

Golive, YR, Zachariah, S., Dubey, R., Chattopadhyay, S., Bhaduri, S., Singh, HK, Bora, B., Kumar, S., Tripathi, A.,

Kottantharayil et al., 2019. Analysis of field degradation rates observed in all-India survey of photovoltaic module reliability 2018. IEEE Journal of Photovoltaics, 10 (2), 560–567. https://doi.org/10.1109/JPHOTOV.2019.2954777.

Fonseca, J.E.F. Fonseca, Oliveira, S. F., Prieb ,C. W. M, Krenzinger A., Degradation Analysis of a photovoltaic generator after operating for 15 years in southern Brazil, Solar Energy Solar Energy Volume 196, 15 January 2020, Pages 196-206

Jordan, D., Kurtz, S., VanSant, K., and Newmiller, J., 2016. Compendium of photovoltaic degradation rates. Progress in Photovoltaics: Research and Applications, 24 (7), 978-989. https://doi.org/10.1002/pip.2744.

Kumar, M. and Kumar, A., 2017a. An efficient parameters extraction technique of photovoltaic models for performance assessment. Solar Energy, 158, 192–206. https://doi.org/10.1016/j.solener.2017.09.046.

Kumar, M. and Kumar, A., 2017b. Performance assessment and degradation analysis of solar photovoltaic technologies: A review. Renewable and Sustainable Energy Reviews, 78, 554–587. https://doi.org/10.1016/j.rser.2017.04.083.

Luo, W., Khoo, Y.S., Hacke, P., Jordan, D., Zhao, L., Ramakrishna, S., Aberle, A.G. and Reindl, T., 2018. Analysis of the long-term performance degradation of crystalline silicon photovoltaic modules in tropical climates. IEEE Journal of Photovoltaics, 9 (1), 266–271. http://dx.doi.org/10.1109/JPHOTOV.2018.2877007

Meyer, E.L. and Van Dyk, E.E., 2004. Assessing the reliability and degradation of photovoltaic module performance parameters. IEEE Transactions on reliability, 53 (1), 83–92. http://dx.doi.org/10.1109/TR.2004.824831.

Nascimento, L. R., Braga, M., Campos, R. A., Naspolini, H. F. and Rüther, R., 2019. Performance assessment of solar photovoltaic technologies under different climatic conditions in Brazil. Renewable Energy, 146, 1070-1082. https://doi.org/10.1016/j.renene.2019.06.160

Piliougine, M., Guejia-Burbano, R., Petrone, G., Sanchez-Pacheco, F., Mora-López, L., and Sidrach-de Cardona, M., 2021a. Parameters extraction of single diode model for degraded photovoltaic modules. Renewable Energy, 164 (C), 674–686. https://doi.org/10.1016/j.renene.2020.09.

Piliougine, M., Oukaja, A., Sidrach-de Cardona, M. and Spagnuolo, G., 2021b. Temperature coefficients of degraded crystalline silicon photovoltaic modules at outdoor conditions. Progress in Photovoltaics: Research and Applications, 29 (5), 558–570. http://dx.doi.org/10.1002/pip.3396.

Rüther, R., 2019. Performance assessment of solar photovoltaic technologies under different climatic conditions in Brazil. Renewable Energy, 146, 1070-1082. https://doi.org/10.1016/j.renene.2019.06.160

Huang, C., and Wang, L., 2018. Simulation study on the degradation process of photovoltaic modules. Energy Conversion and Management, 165, 236–243. https://doi.org/10.1016/j.enconman.2018.03.056.

Ibrahim, H., and Anani, N., 2017. Variations of PV module parameters with irradiance and temperature. Energy Procedia, 134, 276–285. http://dx.doi.org/10.1016/j.egypro.2017.09.617.

Jordan, D. and Kurtz, S., 2013. Photovoltaic degradation rates - an analytical review. Progress in Photovoltaics: Research and Applications, 21 (1), 12-29. https://doi.org/10.1002/pip.1182.

Rüther, R., & Dacoregio, M. M. (2000). Performance assessment of a 2 kWp grid-connected, building-integrated, amorphous silicon photovoltaic installation in Brazil. *Progress in Photovoltaics: Research and Applications*, *8*(2), 257-266.

Rodrigues Junior, J. and Maciel, R. A., 2021. Análise de desempenho do sistema fotovoltaico do campus Fonseca Teles. Projeto de Graduação em Engenharia Elétrica. UERJ.

Sera, D., Teodorescu, R. and Rodriguez, P., 2008. Photovoltaic module diagnostics by series resistance monitoring and temperature and rated power estimation. 2195–2199. https://doi.org/10.1109/IECON.2008.4758297.

Soto, W., Klein, SA, and Beckman, WA, 2006. Improvement and validation of a model for photovoltaic array performance. Solar energy, 80 (1), 78–88. http://dx.doi.org/10.1016/j.solener.2005.06.010.

Soares, D. R. M., Costa Filho, M. A. F., Mattos E. M., Conceição Leonardo L. R. B. 2017. "Photovoltaic Panel Monitoring System". In Proceedings of the 24th International Congress of Mechanical Engineering – COBEM 2017. Curitiba, PR, Brazil.

Tonini B., Spalenza D. C., Emmerick E. A., Almeida G.P.M., Gomes I. M., Lazzari J., Menequini R. S., citty V. F., Moreau G.P., Tesch L., Souza T.S., Pereira M.M.R., Guimarães W.T., 2013. "Influence Of Air Pollution On The Performance Of Photovoltaic Modules in Vitória, Es". Revista Científica Faesa, Vol. 9, No. 1, pp. 81–91.

Vera, Luis Horacio César Wilhelm Massen Prieb e Arno Krenzinger, "comparação do desempenho de módulos fotovoltaicos após seis anos de operação", Universidad Nacional de Nordeste, Departamento de Ingeniería Mecánica, Av. Las Heras nº 727, Resistencia, Chaco, Argentina, Teléfono: +54-3722-420076, Email: lh_vera@yahoo.com.ar, Avances en Energías Renovables y Medio Ambiente Vol. 10, 2006. Impreso en la Argentina. ISSN 0329-5184

Villalva, M., Gazoli, J., and Filho, E., 2009a. Comprehensive approach to modeling and simulation of photovoltaic arrays. Power Electronics, IEEE Transactions on, 24, 1198 – 1208. https://doi.org/10.1109/TPEL.2009.2013862.

Villalva, M.G., Gazoli, J.R., and Ruppert Filho, E., 2009b. Modeling and circuit-based simulation of photovoltaic arrays. In: Brazilian Power Electronics Conference, IEEE, 1244–1254.

8. RESPONSIBILITY NOTICE

The author(s) is (are) the only responsible for the printed material included in this paper.